

ON THE RELATIVE CONTRIBUTIONS OF DYNAMIC AND THERMODYNAMIC FORCING OF SEA ICE CONCENTRATION ANOMALIES IN THE SOUTHERN BEAUFORT SEA INFERRED THROUGH SPATIOTEMPORAL STATISTICAL ANALYSIS.

Jennifer V. Lukovich* and David G. Barber

University of Manitoba, Winnipeg, Manitoba, Canada.

Previous sea ice studies have demonstrated a reduction in sea ice areal extent (Parkinson et al. 1999; Serreze et al. 2003; Johannessen et al. 2004) and thickness (Laxon et al. 2003; Yu et al. 2004). While this behaviour is thought to be a signature of sea ice response to global climate variability and change, it is also directly attributable to sea ice response to dynamic and thermodynamic atmospheric and oceanic forcing mechanisms. Recent sea ice studies of the Southern Beaufort Sea (SBS) for the Canadian Arctic Shelf Exchange Study (CASES) have shown a correspondence between sea-ice concentration (SIC) anomalies and atmospheric forcings (Barber and Hanesiak 2004). The role of coupled atmospheric and oceanic forcing mechanisms in governing sea ice variability has also been examined in the context of coastal upwelling, freshwater transport and variations in the Beaufort gyre (Proshutinsky et al. 2002). Recent modelling studies of summertime ice-edge retreat along the Canadian Shelf of the Beaufort Sea have further demonstrated that wind-driven upwelling is effective in generating shelf/basin exchange when the ice edge retreats beyond the continental shelf break (Carmack and Chapman 2003).

The present study examines this correspondence through the investigation of spatiotemporal autocorrelations for the total sea ice concentration (SIC) anomalies in the SBS, as well as for atmospheric parameters during the onset of ice formation. Temporal autocorrelations are computed for all pixels to yield an e-folding time spatial distribution (EFSD) in the SBS study region. The e-folding time is defined as the time lag at which the autocorrelation is equal to $1/e$, where the autocorrelation for a field ϕ and time lag τ is expressed as

$$R(\tau) = \frac{\langle (\phi(\tau) - \langle \phi \rangle)(\phi(t + \tau) - \langle \phi \rangle) \rangle}{(\phi(t) - \langle \phi \rangle)^2} \quad (1)$$

*Thermodynamic processes are examined through the evaluation of timescales associated with the atmospheric parameter of surface air temperature (SAT). Dynamic processes are examined through the

evaluation of timescales associated with the atmospheric parameters of sea level pressure (SLP), in addition to zonal and meridional winds and their gradients. Moreover, the Weiss criterion, which monitors strain- and relative vorticity-dominated regions, is used to evaluate the influence of shear and cyclonic, namely dynamical, effects associated with the Beaufort gyre on SIC anomaly behaviour. The Weiss criterion Q is expressed as

$$Q = S^2 - \omega^2 \quad (2)$$

Here $S^2 = S_n^2 + S_s^2$ denotes the strain, for $S_n = \partial_x u - \partial_y v$ the stretching rate and $S_s = \partial_x v + \partial_y u$ the shear component of the strain, and $\omega = \partial_x v - \partial_y u$ denotes the relative vorticity. Strain-dominated regions are represented by $Q > 0$ and vorticity-dominated regions by $Q < 0$.

Analyses of the EFSD averaged from years 1979 – 2000 show that SIC anomalies are characterized by a 4 – 7 week timescale to the north and west of Banks Island, and within the eastern extremity of the Amundsen Gulf (Figure 1). These correspond approximately to regions where significant negative SIC anomaly trends were previously detected (Barber and Hanesiak 2004) for this same time period. This correspondence suggests that areas exhibiting a reduction in SIC have a distinct temporal persistence on the order of 4-7 weeks.

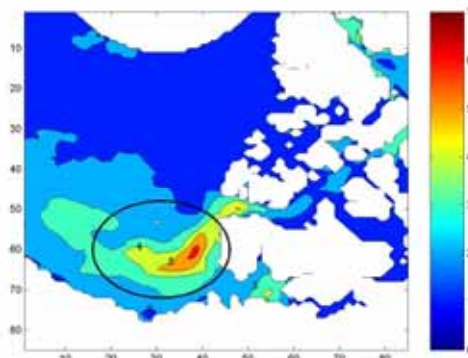


Figure 1. Mean e-folding time spatial distribution (EFSD) for SBS, computed from autocorrelations averaged over 22 years at each pixel with year 1987–1988 excluded due to missing data. Contours are in weeks.

Spectral analysis of SAT, SLP, zonal and meridional winds and their gradients underlines the relationship

* Corresponding author address: Jennifer Verlaine Lukovich, Centre for Earth Observation Science, Faculty of Environment, University of Manitoba, Winnipeg, Manitoba, CANADA. R3L 1T1. email: lukovich@cc.umanitoba.ca

between the 4-7 week timescale in SIC anomalies and dynamical forcing mechanisms in the form of wind gradients (Figure 2). This is illustrated in the existence of peaks at frequencies of approximately 14 weeks^{-1} and 0.25 weeks^{-1} (corresponding to $t = 7$ and $t = 4$ weeks, respectively) for the power spectrum of the Weiss criterion. Power spectra for the dynamical quantities of the meridional and zonal winds, relative vorticity and, to a lesser extent, SLP, also exhibit an accumulation of power in this frequency range. This is in contrast to the thermodynamic quantity of SAT, where most power is concentrated at lower frequencies.

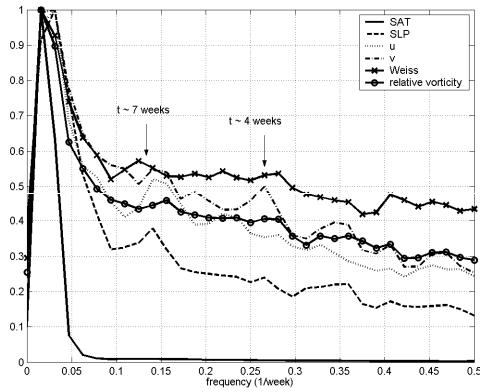


Figure 2 Power spectra averaged over 22 years for SAT, SLP, zonal and meridional winds, Weiss criterion and relative vorticity.

The results from this investigation further suggest a correspondence between strain, a predominance in upwelling-favourable winds and the 4 – 7 week timescale in SIC anomalies. In particular, the prevalence of northeasterly winds to the west of Banks Island (Figure 3) indicate that dynamical forcing mechanisms likely contribute to the observed coherence in EFSD during the onset of ice formation.

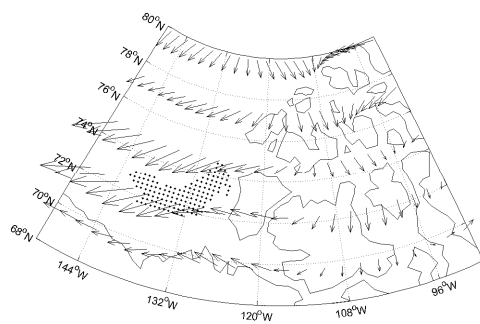


Figure 3 Composite vector wind fields from weeks 1 to 5 averaged over 22 years. The dot pattern indicates the 4-7 week SIC anomaly EFSD grid coordinates contained in ellipse of Figure 1.

Results also show that the mean Weiss criterion (Figure 4) fields exhibit a distinct covariance with the location of the EFSD SIC coherence pattern. In particular, areas located at the periphery of strain-dominated regions established by the neighbouring cyclonic ((144W, 72N)) and anticyclonic ((138W, 75N)) regimes (and located at $\sim(150W, 75N)$) coincide spatially with the 4 – 7 week regime in the SIC anomaly EFSD. Furthermore, the mean Weiss field demonstrates that the average strain rate of the wind field is on the order of $S \sim \sqrt{Q} \sim 10^{-4} \text{ s}^{-1} \sim 2 \text{ hrs}$. We speculate, based on the predominance of upwelling-favorable winds and similarity in the Weiss criterion timescales and spatial pattern to the 4 – 7 week SIC anomaly pattern, that such high-frequency waves work in concert with oceanic mesoscale eddies which have speeds on the order of 0.1 m/s , to generate the observed spatiotemporal pattern in SIC anomalies and hence govern SIC anomaly behaviour.

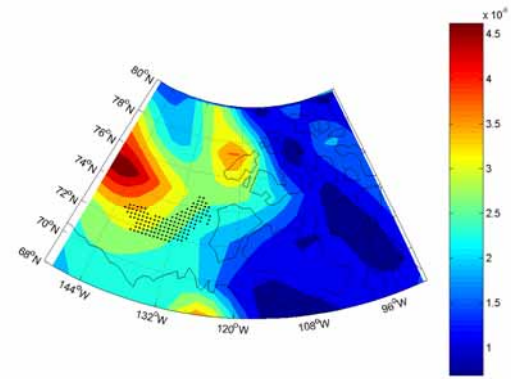


Figure 4 Mean Weiss criterion averaged over 5 weeks from October (week 40) over 22 years. Large positive values indicate strain-dominated regions. Dot pattern indicates the location of the SIC anomaly EFSD coherence pattern.

The relationship between the 4-7 week SIC anomaly timescale, strain-dominated regions and upwelling-favorable winds in the SBS highlight the importance of atmospheric dynamical forcing in governing antecedent sea-ice conditions in the fall of each year. The implications of this work reside also in understanding important connections between atmospheric dynamical forcing and the potential of adding a significant heat source to the base of the sea ice from oceanic upwelling. If confirmed in other studies this connection warrants further attention due to the fact that most of the areal reduction in sea ice is currently occurring at the margins of the landfast sea ice and the mobile pack of the central arctic within flaw lead polynya systems hemispherically (Barber and Massom 2005). Once we understand the processes coupling the ocean and atmosphere in forcing SIC anomalies we can construct more realistic predictive models about how the northern hemispheric

flaw lead polynya system is likely to respond to Arctic climate variability and change.

References

Barber, D.G. and J. Hanesiak. 2004. Meteorological forcing of sea ice concentrations in the Southern Beaufort Sea over the period 1978 to 2001. *J. Geophys. Res.* 109, C06014, doi:10.1029/2003JC002027.

Barber, D.G., and R. Massom. A Bipolar Comparison of Sea Ice and Polynya Dynamics. In: Smith, W.O. and D.G. Barber (eds) *Polynyas: Windows into Polar Oceans*. Elsevier Oceanography Series. In review.

Carmack E.C. and D.C. Chapman (2003), Wind-driven shelf/basin exchange on an Arctic Shelf: the joint roles of ice-cover extent and shelf-break bathymetry, *Geophys. Res. Lett.*, 30(14), doi:10.1029/2003GL017526.

Johannessen O.A. et al. (2004), Arctic climate change: observed and modeled temperature and sea-ice variability, *Tellus*, 56A, 328 – 341.

Laxon S., N. Peacock and D. Smith (2003), High interannual variability of sea ice thickness in the Arctic region, *Nature*, 425, 947 – 949.

Okubo A. (1970), Horizontal dispersion of floatable particles in the vicinity of velocity singularities such as convergences, *Deep-Sea Res.*, 17, 445 – 454.

Proshutinsky A., Bourke R.H. and F.A. McLaughlin (2002), The role of the Beaufort Gyre in Arctic climate variability: Seasonal to decadal climate scales, *Geophys. Res. Lett.*, 29, 15847 – 15851.

Serreze M.C., J.A. Maslanik, T.A. Scambos, F. Fetterer, J. Stroeve, K. Knowles, C. Fowler, S. Drobot, R.G. Barry, and T.M. Haran. (2003), A record minimum arctic sea ice extent and area in 2002, *Geophys. Res. Lett.*, 30, 3, 1110.

Weiss J. (1991), The dynamics of enstrophy transfer in two-dimensional hydrodynamics, *Physica D*, 48, 273 – 294.

Yu Y., G.A. Maykut and D.A. Rothrock (2004), Changes in the thickness distribution of Arctic sea ice between 1958 – 1970 and 1993 – 1997, *J. Geophys. Res.*, 109, C08004, doi: 10.1029/2003JC001982.